

J. Cailloux <sup>a</sup>, J. M. Raquez <sup>b</sup>, G. L. Re <sup>c</sup>, O. Santana <sup>a</sup>,  
P. Dubois <sup>b</sup>, M. Ll. MasPOCH <sup>a</sup>

<sup>a</sup> Centre Català del Plàstic – Universitat Politècnica de Catalunya Barcelona Tech (EEBE-UPC), C/Colom, 114, Terrassa, 08222, Spain

<sup>b</sup> Laboratory of Polymeric and Composite Materials, Center of Innovation and Research in Materials & Polymers (CIRMAP), University of Mons (UMONS), 23 Place du Parc, Mons, B-7000, Belgium

## Procesado en fundido de PLA reforzado con nanofibras de celulosa a partir de un masterbatch preparado de forma sostenible

### RESUMEN

#### Historia del artículo:

Recibido 28 de Mayo 2019

En la versión revisada 15 Junio 2019

Aceptado 1 Julio 2019

Accesible online 15 de Julio 2019

#### Palabras clave:

Poli (ácido láctico)

Poliétilen glicol

Nanofibras de celulosa

Sistema portador

Mezclado en fundido

En este estudio, se fabricaron bionanocompuestos de poli (ácido láctico) (PLA) reforzados con nanofibras de celulosa (CNF) a través de equipos industrialmente escalables. Las diferencias de compatibilidad entre el PLA hidrófobo y la CNF hidrófila se contrarrestaron utilizando un masterbatch de polietilenglicol (PEG) / CNF en base agua, minimizando así la autoaglomeración de la CNF durante el secado. Por microscopía de luz polarizada se mostró un refinamiento progresivo de la distribución de la CNF en el PLA a medida que aumenta el contenido de PEG. La eficiencia del sistema portador de PEG se corroboró mediante ensayos reológicos. Se destaca la formación de fuertes interacciones de la CNF o una red tridimensional de CNF para los compuestos basados en masterbatch que contienen 20% en peso de PEG, lo que corrobora el éxito de nuestro enfoque sostenible para dispersar efectivamente CNF a través de técnicas de mezclado en fundido. Bajo carga termomecánica, la estructura rígida de la CNF dominó la respuesta viscoelástica de los compuestos plastificados, demostrando la capacidad de carga, tanto en el estado vítreo como en el gomoso, de la CNF cuando está bien distribuida. Este método rápido y sencillo es adecuado para la preparación de masterbatches de CNF procesables en fundido, que puede ser utilizado por los métodos convencionales de procesamiento a escala industrial.

## Melt Processing of Cellulose Nanofibers Reinforced PLA from a Sustainable Masterbatch Process

### ABSTRACT

#### Keywords:

Poly(lactic acid)

Polyethylene glycol

Cellulose nanofibers

Carrier system

Melt blending

In this study, cellulose nanofiber (CNF)-reinforced poly (lactic acid) (PLA) bionanocomposites were manufactured through industrially scalable equipments. The compatibility differences between hydrophobic PLA and hydrophilic CNF was counteracted using a water-based polyethylene glycol (PEG)/CNF masterbatch approach, hence minimizing CNF self-agglomeration during drying. Polarized light microscopy showed a progressive refinement of the CNF distribution into PLA upon increasing the PEG content. Rheological experiments provided further evidences about the efficiency of the PEG carrier system. Indeed the formation of strong CNF interactions or a three-dimensional CNF network was highlighted for the masterbatch-based composites holding 20 wt.% of PEG, corroborating the successfulness of our sustainable approach to disperse effectively CNF through melt blending techniques. Under thermo-mechanical loading, the rigid percolated CNF structure mastered the viscoelastic response of the plasticized composites, demonstrating the load-bearing capacity of well-entangled CNF in the glassy as well as in the rubbery state. This rapid and straightforward physical method is a suitable approach for preparing dried and concentrated melt-processable CNF masterbatches that can be adopted in conventional melt-processing methods at an industrial scale.

## 1 Introduction

Over the past decades, much research has been focussed on the development of cellulose reinforced poly(lactic acid) (PLA) nanocomposites. This is due to the need of fully bio-based materials with a more environmentally friendly life cycle [1]. Among all cellulose-based nanoreinforcements, cellulose nanofibers (CNF) got into the focus of investigation as reinforcement material for applications in food packaging, automotive, construction, among others [2]. This is due to their large aspect ratio, together with their outstanding mechanical properties and their low percolation threshold. Numerous works reported that CNF loadings as low as 0.5 to 5 wt.% can positively influence PLA thermal, mechanical, rheological and foaming properties [3, 4].

Nonetheless, the well-established self-agglomeration issues of cellulose-based materials into polymers restrict the full CNF development to specific processing methods. Recall that CNF are obtained as a hydrophilic gel-like suspension. Accordingly, solvent casting/evaporation from a liquid medium is nowadays the frontrunner technique to obtain a satisfactory CNF dispersion degree, leading to a percolating network at relatively low contents (0.5-1 wt.%) [2, 3]. The modification of the CNF surface is another route to enhance filler dispersion as well as compatibility with the polymeric matrix [5]. However, both methodologies are organic solvent-dependent and time expensive, hence limiting their expansion for mass production.

To overcome these shortcomings, the production of PLA/CNF composites through conventional melt-processing methods is under investigation [6, 7]. Although these methods are faster and solvent-free, CNF aggregation and degradation issues have been reported. Additionally, the continuous shearing applied during processing prevents the formation of a percolating network and higher CNF contents are needed to obtain similar properties as compared to their solvent casting counterparts. In order to provide solutions to CNF aggregation on drying before extrusion, Kiziltas *et al.* [8] reported the use of a masterbatch prepared through melt-blending as carrier system to introduce CNF into PLA. The aqueous suspension of CNF is first melt mixed with a third polymer (polyhydroxybutyrate, PHB) and then the resulting masterbatch is diluted into PLA. Despite that a satisfactory CNF dispersion was observed in the sample holding 5 wt.%, the masterbatch preparation through melt blending is somewhat hazardous (CNF wet feeding into PHB at 170 °C). Furthermore, the hydrophobicity of PHB can hinder hydrophilic fillers from dispersing well in the masterbatch.

Our effort to overcome the abovementioned shortcomings focused on the use of a biodegradable water-soluble biopolymer as carrier system (i.e. polyethylene glycol, PEG), that can be rapidly and straightforwardly melt-blended with PLA. The cellulose nanocrystal surface physical PEGylation has already reported as a successful technique to avoid CNF self-agglomeration on drying [9, 10]. However, to the best of the author's knowledge, no researches have been conducted to investigate the effect of a PEG carrier system on the CNF dispersion using industrial scalable melt-processing techniques. Accordingly, this study aimed at investigating the evolution of the dispersion of 5 wt.% of CNF into PLA nanocomposites using different percentages of PEG (0, 10 and 20 wt.%) as carrier system through microscopy and rheological

analyses. Finally, the load-bearing capacity of CNF was studied via thermo-mechanical experiments.

## 2 Experimental section

### 2.1 Materials

An extrusion grade polylactic acid (Ingeo PLA 4032D, D-lactic content  $\approx$  2%) was supplied by Natureworks LLC (Arendonk, Belgium) and used as received. Polyethylene glycol (PEG) (MW  $\approx$  2000 g.mol<sup>-1</sup>) was purchased from Alfa Aesar (ThermoFisher, Karlsruhe, Germany). An antioxidant (Irganox 1010) was kindly supplied by BASF (Barcelona, Spain) to counteract PLA degradations during melt blending. Enzymatic-cellulose nanofibers (CNF) were kindly supplied by the Chalmers University of Technology [11]. The diameter distribution of the nanofibrils was about 11.5 nm  $\pm$  4.0 nm [12].

### 2.2 PLA/PEG/CNF nanocomposites processing

Initially, two PEG-based masterbatches with a nominal content of dried CNF set at 20 and 33 wt.% were prepared by dissolving PEG in distilled water at room temperature. Then a desired content of the the gel-like suspension of CNF was added to the solution and stirred for 3h at RT. The final mixtures were poured onto glass Petri dishes and dried at 35°C for 3 days. For comparison purposes, CNF alone were subjected to the same experimental protocol.

The obtained flakes of the different PEG-based masterbatches were melt blended with PLA using a DSM Xplore Micro 15cc twin screw compounder to reach a CNF nominal content of 5 wt.%. The melt temperature was set to 180°C, the screw speed at 100 rpm and the residence time was fixed at 2.5 min under a N<sub>2</sub> blanket. Prior to processing, PLA pellets were vacuum-dried at 60°C overnight. During mixing, 0.5 wt.% of Irganox 1010 was added to minimize PLA degradation. The nominal PLA/PEG/CNF ratios were 95/0/5; 85/10/5 and 75/20/5 and the samples were codified as PLA/CNF, PLA/10PEG/CNF and PLA/20PEG/CNF, respectively.

Rectangular (45 x 12 x 2 mm) and disk-shaped (diameter: 25 mm; thickness: 1.5 mm) samples were prepared by injection-moulding using a DSM Xplore Micro 5cc injection moulding machine with a barrel temperature of 190°C and a mold temperature of 30°C. Reference PLA and PLA/PEG blends (nominal ratios: 90/10 and 80/20 wt/wt) were prepared using the same processing procedure for the sake of comparison.

### 2.3 Characterization

Optical microscopy (Nikon, Optiphot-Pol XTP-11) equipped with a cross-polarizer was used to evaluate the effect of the PEG content on the degree of CNF dispersion within PLA. DSC analyses were carried out using a MDSC Q2000 instrument (TA Instruments) under a dry N<sub>2</sub> atmosphere. 5-6 mg of the samples were sealed in standard aluminium pans and subjected to a heating/cooling/heating procedure over a temperature range from -80 to 200 °C at a heating/cooling rate of 10 °C.min<sup>-1</sup>. The degree of crystallinity (X<sub>c</sub>) was calculated using a melting enthalpy for a 100% crystalline PLA of 93.6 J.g<sup>-1</sup> [13].

The possible thermal degradation of CNF was evaluated via wide angle X-ray scattering analysis using a Bruker D8



Advance diffractometer (Billerica) with  $\text{CuK}\alpha$  radiation of wavelength of 0.154 nm. Scans were recorded in the range 5–50° (step size= 0.02, scanning speed= 1 s/step).

The rheological behaviour was evaluated using an AR-G2 rheometer (TA Instruments) in parallel plate (25 mm) configuration with a constant gap of 1.4 mm at 180 °C under a dry  $\text{N}_2$  atmosphere. SAOS tests were carried out in the angular frequency range  $1 < \omega < 623 \text{ rad}\cdot\text{s}^{-1}$  at a fixed 3% strain (L.V.R.). To ensure sufficient data in the terminal regime, creep-recovery experiments were performed using fresh samples. The dynamical mechanical spectra were obtained combining the results from both methodologies.

Dynamic mechanical thermal analysis (DMTA) was performed on rectangular samples using a DMTA Q800 equipment (TA Instruments). Samples were tested in dual cantilever bending mode from -100 to 80°C at a heating rate of  $2^\circ\text{C}\cdot\text{min}^{-1}$  at 0.02% of deformation (L.V.R.) and a frequency of 1 Hz.

### 3 Results and discussion

After melt-processing, the CNF dispersion within PLA was investigated using cross-polarized light microscopy and the micrographs are depicted in **Figure 1**. PLA/CNF sample revealed the expected coarse suspension of large CNF aggregates, which is in line with the well documented self-agglomeration issue of CNF on drying before melt blending [14].

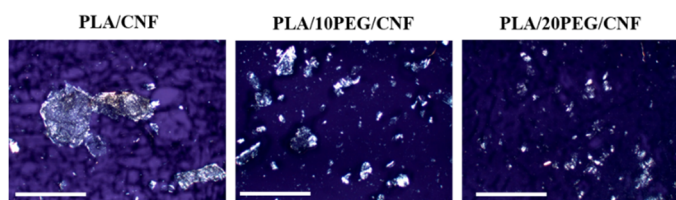


**Figure 1.** Cross-polarized light micrographs highlighting a gradual size reduction of the CNF aggregates within PLA upon increasing the PEG content. The regions exhibiting a strong birefringence show CNF aggregates. (Scale bars = 1 mm).

In contrast, a more homogeneous morphology was seemingly obtained for both PLA/PEG/CNF bio-composites. Polarized light microscopy evidenced the presence of a larger number of smaller CNF aggregates whose size apparently gradually decreased when CNF were pre-mixed with PEG first and then melt blended with PLA. Accordingly, the ability of PEG to reduce CNF aggregation through the masterbatch approach suggested that PEG acted as dispersant.

The thermal properties of injected samples obtained from the first heating scan are compiled in **Table 1**. The incorporation of CNF alone did not modify the PLA thermal behaviour. Both samples can be considered as amorphous. The plasticizing effect attributed to low MW PEG on PLA led to a clear improvement of the PLA/PEG blend crystallization ability [15]. The cold crystallization temperature ( $T_{cc}$ ) decreased while  $X_c$  increased with the PEG content. Interestingly, the melt temperature ( $T_m$ ) remained almost constant. According to the processing conditions used, adding CNF did not greatly influence PLA/PEG thermal behaviour.

The second heating scan revealed that PEG is only partially miscible within PLA when adding 20 wt.% PEG. The measured  $X_c$  values of PLA and PLA/CNF samples indicated that

aggregated CNF did not improve the poor crystallization ability of PLA. By contrast,  $X_c$  values increased up to 16 % between PLA/10PEG and PLA/10PEG/CNF samples, suggesting that an improvement in the CNF dispersion could enhance PLA crystallization. Indeed, their large specific area could enhance the heterogeneous crystallization of PLA [2]. Such effect was not clearly identified between samples with 20 wt.% of PEG, possibility due to an advanced plasticizing effect.

**Table 1.** DSC data obtained from the first heating scan.

Sample nomenclature	$T_g$ (°C)	$T_{cc}$ (°C)	$T_m$ (°C)	$X_c$ (%)
PLA	60	108.5	167.6	4
PLA/CNF	61	107.7	167.6	2
PLA/10PEG	- *	75.7	165.9	22
PLA/10PEG/CNF	- *	76.9	166.0	19
PLA/20PEG	- *	88.1	166.9	32
PLA/20PEG/CNF	- *	87	166.8	29

\*Signal overlaps with the melting transition of PEG

Figure 2 shows the X-ray diffractograms of dried CNF and all the CNF-reinforced (nano)composites. Dried CNF show peaks around  $2\theta = 9.7, 15.1, 16.2$  and  $22.5^\circ$ , which are characteristic of the semi-crystalline cellulose I structure [16]. Since the peak intensity correlates with the crystallinity degree, a qualitative evaluation of the CNF crystallinity can be done by comparing the magnitude of the diffraction peak at  $2\theta = 22.5^\circ$  between dried CNF and CNF-reinforced composites, as shown in **Figure 2**. Results suggested that melt processing showed a lower effect on the original integrity of cellulose I crystal polymorphism when the CNF surface was PEGylated first.

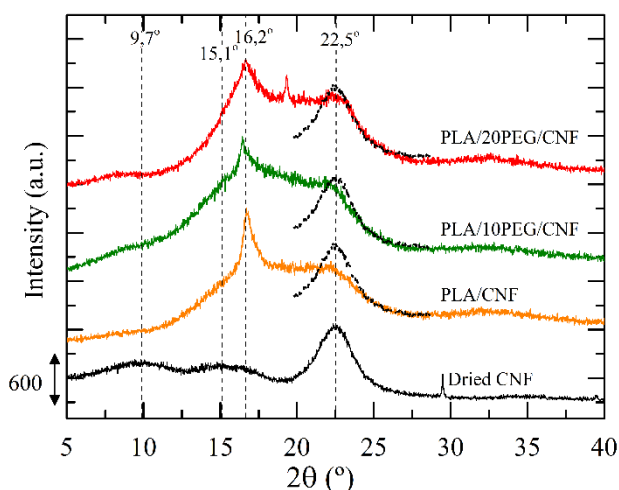


**Figure 2.** XRD diffraction patterns of dried CNF and all the CNF-reinforced samples. The diffraction peak at  $2\theta = 22.5^\circ$  of dried CNF was superimposed with CNF-reinforced material patterns to compare qualitatively the CNF crystallinity degree.

The rheological behaviour of the CNF-reinforced samples were investigated to have an insight in the evolution of the CNF dispersion as a function of the PEG content. **Figure 3** shows the frequency dependence of the complex viscosity,  $|\eta^*|$ , together with the Van-Gurp Palmén plots where the phase angle  $\delta = \arctan(G''/G')$  is plotted against the complex modulus,  $G^*$ .



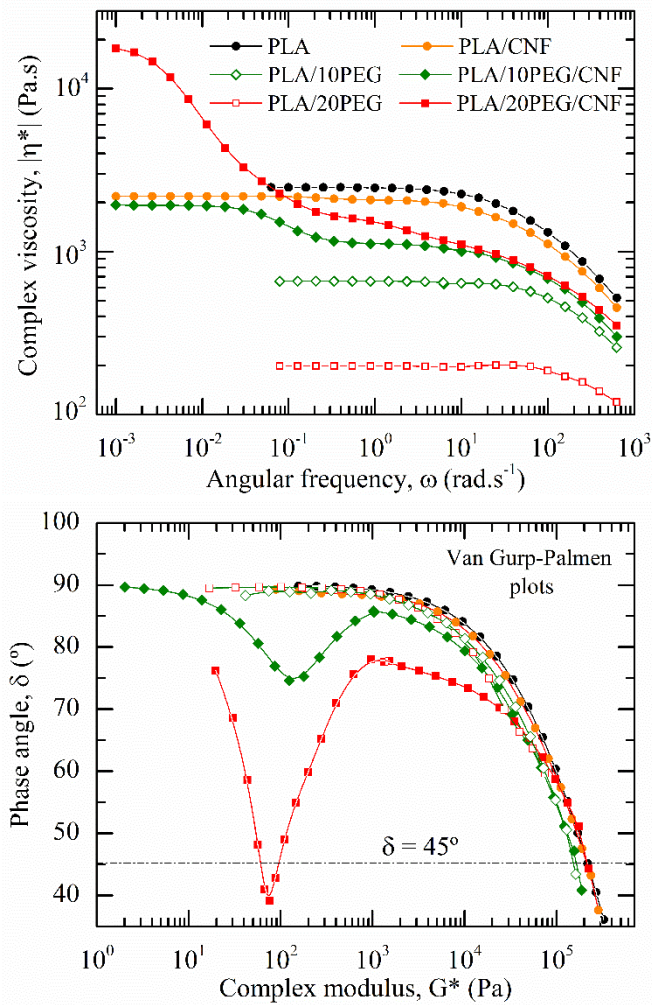


**Figure 3.** Angular frequency dependence of the complex viscosity and the Van Gorp-Palmen Plots for all samples.

Pure PLA exhibits the typical pseudoplastic fluid behaviour. By adding PEG, a gradual drop in  $|\eta^*|$  values was observed due to its plasticizing effect on PLA. PLA/CNF composites exhibited a lower viscosity than PLA over the whole experimental window. This behaviour might be explained by a possible disruption of the molecular network induced by the large CNF aggregates that lower the PLA viscous resistance

Drastic changes in the PLA/CNF rheological behaviour were observed when CNF were added to PLA via the PEG masterbatch approach. Both PLA/PEG/CNF samples exhibited the characteristic rheological behaviour of structured fluids. The magnitude of the yield stress in  $|\eta^*(\omega)|$  increased with the PEG content, suggesting that a stronger CNF network was formed in PLA/20PEG/CNF. These observations are supported by the Van Gorp-Palmen plots. While a purely viscous behaviour is characterized by  $\delta=90^\circ$ , a purely elastic melted material exhibits a  $\delta$  value of  $0^\circ$ . The PLA/20PEG/CNF sample displays  $\delta$  values lower than  $45^\circ$ , implying that the elastic component of the melt exceeded the viscous one. This transition is characteristic of solid-like composites and corroborates the formation of a three-dimensional CNF network, also defined as rheological percolating CNF network in PLA/20PEG/CNF samples [17]. This results proves the successfulness of the CNF surface PEGylation to promote filler dispersion within PLA through melt blending.

The effect of the CNF dispersion degree within PLA on the thermo-mechanical properties was investigated through DMTA. **Figure 4** displays the temperature variation of the storage modulus,  $E'$ . **Table 2** compiles the  $E'$  at  $25^\circ\text{C}$ , the minimum  $E'$  value in the rubbery plateau and the  $\alpha$ -relaxation temperature,  $T_{\alpha}$ .

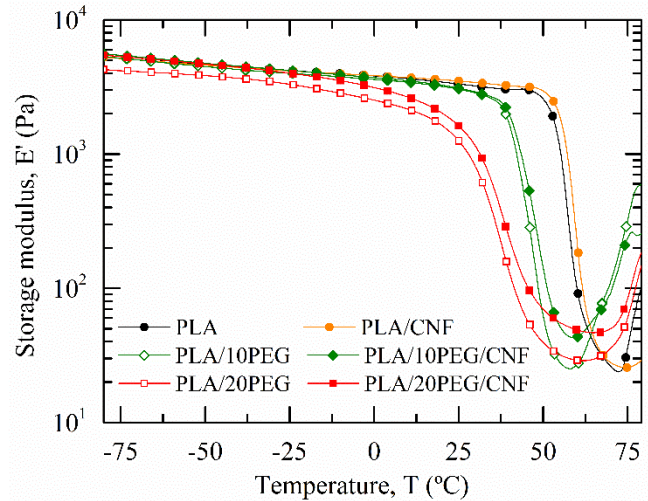


**Figure 4.** Temperature dependence of the storage modulus,  $E'$ .

Pure PLA exhibited the typical behaviour of amorphous polymers. At low temperatures, the sample stiffness remained fairly constant before experimenting a significant drop around  $60^\circ\text{C}$  due to the glassy-to-rubbery transition. This transition is related to the  $\alpha$ -relaxation of the macromolecular chains and corresponds to the dynamic glass transition temperature ( $T_g$ ) of PLA [18]. The incorporation of CNF alone into PLA did not modify neither the temperature dependence of  $E'$  nor the  $T_g$  of PLA within the experimental error, as listed in **Table 2**.

**Table 2.** DMTA results.

Sample nomenclature	$E'$ at $-25^\circ\text{C}$ (GPa)	$E'$ in the RP (MPa) <sup>a</sup>	$T_{\alpha}$ ( $E''$ ) ( $^\circ\text{C}$ ) <sup>b</sup>
PLA	$4.1 \pm 0.3$	$24 \pm 2$	$54 \pm 2$
PLA/CNF	$4.2 \pm 0.1$	$22 \pm 5$	$55.9 \pm 0.2$
PLA/10PEG	$3.8 \pm 0.2$	$28 \pm 3$	$41.3 \pm 0.4$
PLA/10PEG/CNF	$4.3 \pm 0.2$	$38 \pm 3$	$41.4 \pm 0.6$
PLA/20PEG	$3.7 \pm 0.5$	$28 \pm 1$	$27 \pm 1$
PLA/20PEG/CNF	$3.9 \pm 0.2$	$49 \pm 4$	$29 \pm 1$

<sup>a</sup> minimum  $E'$  value in the rubbery plateau (RP).

<sup>b</sup>  $T_{\alpha}$  was determined as the point where the loss modulus,  $E''$ , reached a maximum.

By adding PEG, a clear reduction of the elastic-like behaviour of PLA was reported (lower  $E'$  values). The plasticizing effect of PEG on PLA was evidenced by a progressive decrease in  $T_g$ . From **Figure 4** and **table 2**, it is evident that the advanced plasticization of both PLA/PEG blends suppressed the load bearing contribution of the crystalline phase above  $T_g$ , which could increase the  $E'$  values in the rubbery region [19].

When CNF and PEG were premixed and then melt blended with PLA, both biocomposites exhibited higher  $E'$  values in the glassy region in comparison with their PLA/PEG counterpart.  $E'$  at  $-25^\circ\text{C}$  of PLA/10PEG/CNF sample exceeded equally that of pure PLA. In the rubbery region, the previous CNF surface



PEGylation resulted in a gradual increase of the rubbery storage modulus as compared to unfilled PLA or PLA/CNF samples. For instance, the minimum  $E'$  value in the rubbery plateau increased by 51 % between PLA/20PEG and PLA/20PEG/CNF samples. This enhancement of the sample stiffness above  $T_g$  was ascribed to the tangling effects produced by the internal three-dimensional CNF network which demonstrated the load-bearing capacity of well-entangled CNF [20]. Regarding the PLA/20PEG/CNF sample, a slight increase in  $T_g$  was evidenced as compared to PLA/20PEG sample. This was ascribed to the formation of a percolated CNF network that restricted the molecular mobility of PLA macromolecules [2].

## 4 Conclusions

In the present study, bionanocomposites based on CNF as nanofillers and PLA as polymeric matrix were successfully and straightforwardly prepared through melt processing using a PEG/CNF masterbatch approach. A water-based hydrophilic PEG carrier system was used to counteract the affinity difference between the hydrophobic PLA and hydrophilic CNF, hence minimizing their self-agglomeration on drying. Different PEG concentrations were considered in order to investigate their effect on the final CNF dispersion degree. Finally, surface PEGylated CNF were diluted into PLA using a micro-compounder. Through rheological testing, a clear liquid-solid transition was observed by the masterbatch-based composites holding 20 wt.% of PEG, corroborating the creation of a well-entangled CNF network. Microscopy images confirmed the beneficial effect of an increasing PEG content in achieving a more homogenous morphology. Thermal analysis showed that PEG acted as plasticizer and enhanced the crystallinity of the matrix. However, under the processing conditions used in this work, adding CNF did not impact significantly the final thermal properties. Under thermo-mechanical loading, the elastic response of the rigid interconnected CNF structure mastered the viscoelastic response of the plasticized composites, notably improving PLA rigidity in the glassy as well as in the rubbery state. These promising results showed that PEG can be used as a successful carrier system in order to prepare a highly concentrated CNF masterbatch which then can be rapidly melt-processed using industrial melt-processing technique.

## Acknowledgements

The authors acknowledge the financial support from the Spanish Ministry of Economy and Competitiveness through the Project MAT2016-80045-R (AEI/FEDER,UE). BASF is thanked for kindly supplying Irganox 1010<sup>®</sup>. J.-M. Raquez as a FRS-FNRS research associate and LPCM is much indebted to both Wallonia and the European Commission "FSE and FEDER" for financial support in the frame of H2020-LCFM portfolio.

## References

- [1] M. A. S. Azizi Samir, F. Alloin, *et al.*, *Biomacromolecules*, **6**, 2, pp. 612-26 (2005)  
<https://doi.org/10.1021/bm0493685>
- [2] F. Safdari, D. Bagheriasl, *et al.*, *Polym Composite*, **39**, 5, pp. 1752-62 (2018)

<https://doi.org/10.1002/pc.24127>

- [3] W. Ding, T. Kuboki, *et al.*, *Rsc Adv*, **5**, 111, pp. 91544-57 (2015)  
<https://doi.org/10.1039/C5RA16901A>
- [4] S. Y. Cho, H. H. Park, *et al.*, *Macromol Res*, **21**, 5, pp. 529-33 (2013)  
<https://doi.org/10.1007/s13233-013-1057-y>
- [5] K. Missoum, M. Belgacem, *et al.*, *Materials*, **6**, 5, pp. 1745-66 (2013)  
<https://doi.org/10.3390/ma6051745>
- [6] D. Bondeson, K. Oksman, *Compos Interface*, **14**, 7-9, pp. 617-30 (2007)  
<https://doi.org/10.1163/156855407782106519>
- [7] A. P. Mathew, K. Oksman, *et al.*, *J Appl Polym Sci*, **97**, 5, pp. 2014-25 (2005)  
<https://doi.org/10.1002/app.21779>
- [8] A. Kiziltas, B. Nazari, *et al.*, *Carbohydrate polymers*, **140**, pp. 393-9 (2016)  
<https://doi.org/10.1016/j.carbpol.2015.12.059>
- [9] D. Cheng, Y. Wen, *et al.*, *Carbohydrate polymers*, **123**, pp. 157-63 (2015)  
<https://doi.org/10.1016/j.carbpol.2015.01.035>
- [10] P. Zhang, D. Gao, *et al.*, *J Appl Polym Sci*, **134**, 14, pp. (2017)  
<https://doi.org/10.1002/app.44683>
- [11] M. Henriksson, G. Henriksson, *et al.*, *Eur Polym J*, **43**, 8, pp. 3434-41 (2007)  
<https://doi.org/10.1016/j.eurpolymj.2007.05.038>
- [12] G. Lo Re, J. Engstrom, *et al.*, *ACS Applied Nano Materials*, pp. (2018)  
<https://doi.org/10.1021/acsnm.8b00376>
- [13] R. Hakim, J. Cailloux, *et al.*, *J Appl Polym Sci*, pp. (2017)  
<https://doi.org/10.1002/app.45367>
- [14] Y. Peng, D. J. Gardner, *et al.*, *Cellulose*, **19**, 1, pp. 91-102 (2012)  
<https://doi.org/10.1007/s10570-011-9630-z>
- [15] F. J. Li, S. D. Zhang, *et al.*, *Polym Advan Technol*, **26**, 5, pp. 465-75 (2015)  
<https://doi.org/10.1002/pat.3475>
- [16] A. D. French, *Cellulose*, **21**, 2, pp. 885-96 (2014)  
<https://doi.org/10.1007/s10570-013-0030-4>
- [17] J. Stokes, J. Telford, *J Non-Newton Fluid*, **124**, 1-3, pp. 137-46 (2004)  
<https://doi.org/10.1016/j.jnnfm.2004.09.001>
- [18] L. Xiao, Y. Mai, *et al.*, *Journal of Materials Chemistry*, **22**, 31, pp. 15732-9 (2012)  
<https://doi.org/10.1039/C2JM32373G>
- [19] T. Tabi, I. Sajó, *et al.*, *Express Polym Lett*, **4**, 10, pp. (2010)  
<https://doi.org/10.3144/expresspolymlett.2010.80>
- [20] M. A. Saïd Azizi Samir, F. Alloin, *et al.*, *Macromolecules*, **37**, 11, pp. 4313-6 (2004)  
<https://doi.org/10.1021/ma035939u>

